Journal of Sol-Gel Science and Technology (2023) 108:112–119
https://doi.org/10.1007/s10971-023-06180-0

ORIGINAL PAPER: NANO-STRUCTURED MATERIALS (PARTICLES, FIBERS, COLLOIDS, COMPOSITES, ETC.)

Construction of SnO_2/MWCNT nanocomposites as electrode materials for supercapacitor applications

P. Jayanthi[1,2] · G. Saranya[1] · J. Duraimurugan[3] · Prabhu Sengodan[4] · Siranjeevi Ravichandran[5] · R. Usha[4] · N. Bhuvaneshwari[1]

Received: 1 March 2023 / Accepted: 23 June 2023 / Published online: 11 July 2023

Abstract

Both transition-metal oxide and carbon-based nanocomposites play important roles in the electrochemical properties. The rational design of carbon-based transition-metal oxides could accelerate the electrochemical double layer and Faradaic redox reaction kinetics, which increases the electroactive sites in the supercapacitor applications. Here, we synthesized SnO_2/MWCNT nanocomposite through a simple hydrothermal method and used it as electrode material for energy storage applications. The physiochemical characterization was tested by using various techniques such as XRD, FT-IR, FE-SEM, and TEM. The SnO_2/MWCNT electrode material delivered a maximum specific capacitance of 255 F/g at 2 A/g and 93% of capacitance retention after 1000 GCD cycles at 10 A g^{-1} in an alkaline medium.

Graphical Abstract

Fig. Schematic diagram of SnO_2/MWCNTs nanocomposite with electrochemical performances. Here, we synthesized SnO_2/MWCNT nanocomposite through a simple hydrothermal method and used as electrode material for energy storage application. The SnO_2/MWCNT electrode material delivered maximum specific capacitance of 255 F/g at 2 A/g.

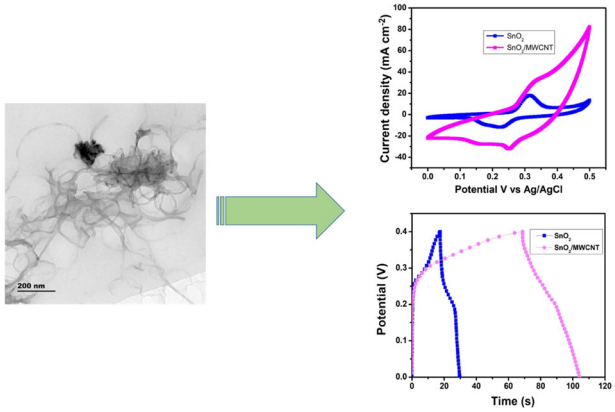

✉ N. Bhuvaneshwari
drbhuvaneshwari1976@gmail.com

[1] Department of Chemistry, Chikkaiah Naicker College, Erode, Tamil Nadu, India

[2] Department of chemistry, K.S.R. College of Engineering (Autonomous), Tiruchengode 637 215 Tamil Nadu, India

[3] Department of Physics, K.S. Rangasamy College of Arts and Science (Autonomous), Tiruchengode 637 215 Tamil Nadu, India

[4] Department of Physics, Saveetha School of Engineering, Saveetha Institute of Medical and Technical Sciences, Saveetha University, Chennai 602 105 Tamil Nadu, India

[5] Department of Chemistry, Saveetha School of Engineering, Saveetha Institute of Medical and Technical Sciences, Saveetha University, Chennai 602 105 Tamil Nadu, India

Keywords SnO_2 · MWCNT · Electrochemical experiments · Supercapacitors

1 Introduction

The escalating environmental pollution and the world's energy crisis have encouraged the creation of secure and effective energy storage technologies [1]. Supercapacitors (SCs), fuel cells (FCs), and batteries (Bts) are potentially excellent examples of energy storage/conversion that have attracted a lot of interest from both industry and research [2–4]. Particularly, SCs, often referred to as electrochemical capacitors or ultracapacitors, are presently being lauded as extremely effective and pollution-free physical energy storage devices [5]. Based on the energy storage techniques, there are two types of SCs: pseudo capacitors (PCs) and electric double-layer capacitors (EDLCs) [6]. Charges are stored on the electrode and electrolytic contact in pseudo capacitors (PCs) using a faradaic mechanism [7]. The metal oxides (NiO, SnO_2, Co_3O_4, MnO_2, TiO_2, etc.), metal sulfides (NiS, CuS, CoS, MoS_2, etc.), and conducting polymers (Polyaniline, Polypyrrole, etc.) have pseudocapacitive behaviors [8–10].

Charges from EDLCs build up at the electrode/electrolyte contact as a result of the formation of electric double layers. Graphene, carbon nanotubes (CNT), and activated carbon (AC) are examples of members of the carbon family that can be employed as EDLC materials [11, 12]. Because of the quick, reversible Faradaic redox reaction of the electrode material in the electrolyte solution, the PCs can store more energy than EDLCs. The volumetric energy density of SCs is still far off, which limits their applicability [13].

Moreover, SnO_2 is receiving a lot of attention for use in supercapacitors due to its several oxidation states, wide potential window, low price and eco-friendly composition, and high theoretical capacity (782 mA h g^{-1}) [14]. However, due to their poor stability, low electrical conductivity, and quick capacitance decrease, their single metal oxide-based anode materials have demonstrated poor electrochemical performance. To enhance the electrochemical characteristics, these hybrids based on binary or mixed metal oxides are being investigated. For example, Ahmed et al. reported that activated carbon waste (ACW) and the impregnation of a SnO_2 nanocomposite electrode exhibited a superior specific capacitance of 30.46 F/g at 0.122 A/g in the neutral Na_2SO_4 [15]. Recently, Asaithambiet al. reported that the Mn-doped SnO_2/MoS_2 composite showed a remarkable specific capacitance of 242 F/g at 0.5 A/g and life cycle performance of 83.95% after 5000 continuous GCD cycles [16]. However, there are efficient other methods to produce high-performance cathode materials for supercapacitors, such as metal oxide with carbon material composites.

Herein, we report SnO_2/MWCNT hybrids as anode materials synthesized by a one-step hydrothermal method for supercapacitor application. With excellent cycle-life stability (93 percent retention after 1000 cycles at 10 A/g), the calculated specific capacitance was found to be 255 F/g at 2 A/g.

2 Experimental methods

2.1 Chemicals

Tin chloride pentahydrate ($SnCl_4{\cdot}5H_2O$, 99%), sodium hydroxide (NaOH, 99%), and multiwalled carbon nanotubes ((MWCNT) 98.5%, length (1 to 10 μm)). All the chemicals were purchased from Merck (India) and chemicals were used without further purification.

2.2 Synthesis of SnO_2 nanostructures

In the typical synthesis of SnO_2 nanostructures, 0.1 M of $SnCl_4{\cdot}5H_2O$ and 0.2 M of NaOH were subsequently dissolved in 50 mL of mixed solution de-ionized water under magnetic stirring. The final homogenous solution was put into a 100 mL Teflon-lined stainless steel autoclave and heated in an electrical oven for 24 h at 160 °C. The product was then filtrated and dried at 60 °C for more than 24 h.

2.3 Synthesis of SnO_2/MWCNT nanocomposites

The SnO_2/MWCNT nanocomposites were prepared by the hydrothermal method. As-purchased multiwalled carbon nanotubes (MWCNT) 100 mg was dispersed into 50 mL deionized water with ultrasonication for 2 h. After that, 0.1 M of $SnCl_4{\cdot}5H_2O$ and 0.2 M of NaOH were subsequently dissolved in 50 mL of the mixed above solution. After that, the solution was moved into the Teflon-lined stainless steel autoclave and heated at 160 °C for 24 h. The final product was dried at 80 °C in the electrical oven overnight.

2.4 Material characterization

X-ray powder diffractometer (XRD) Rigaku (Cu-Kα radiation), High resolution scanning electron microscope (HR-SEM, Magellan 400 L), HRTEM (JEOL, JEM-2100F, performing at 200 kV), and FT-IR technique (FT-IR, NEXUS 470).

2.5 Electrochemical measurements of a three-electrode cell

The electrochemical energy storage performance of prepared electrodes was studied by a 3 M aqueous KOH electrolyte in three electrodes cell set-up. The standard three-electrode configuration included a nickel-foam-based working electrode, Ag/AgCl as a reference electrode, and graphite rod as a counter electrode. The active material (80 weight percent), activated carbon (10 weight percent), and polyvinylidene fluoride (10 weight percent) were mixed with the help of a mortar and pestle, and three drops of N-Methyl-2-pyrrolidone (NMP), an organic solvent, to make a slurry. The slurry was coated in Ni foam (2 × 1) surfaces and dried vacuum oven at 60 °C for 12 h. The cyclic voltammetry (CV), galvanostatic charge-discharge (GCD), and electrochemical impedance spectroscopy (EIS) were measured by using an electrochemical workstation (Squidstat Potentiostats- United States).

The GCD plots were used to estimate the specific capacitance (C_{sp}) of working electrodes as follows,

$$C_{sp} = \frac{I * \Delta t}{\Delta m * \Delta V} \quad (1)$$

Where I, Δt, ΔV, and m indicate the applied current (A), discharge time (s), area of discharging time, working

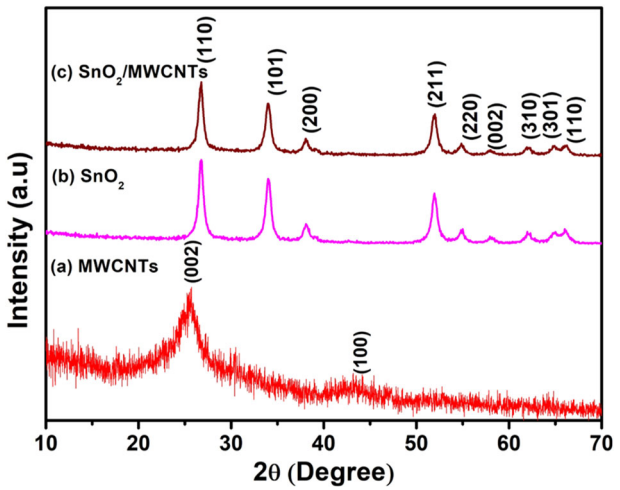

Fig. 1 Powder XRD patterns of (**a**) MWCNTs, (**b**) SnO_2, and (**c**) SnO_2/MWCNT nanocomposite

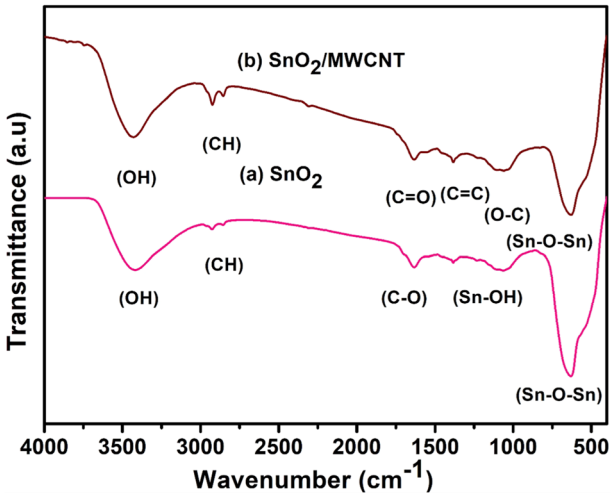

Fig. 2 FT-IR of nanostructured (**a**) SnO_2, and (**b**) SnO_2/MWCNT composites

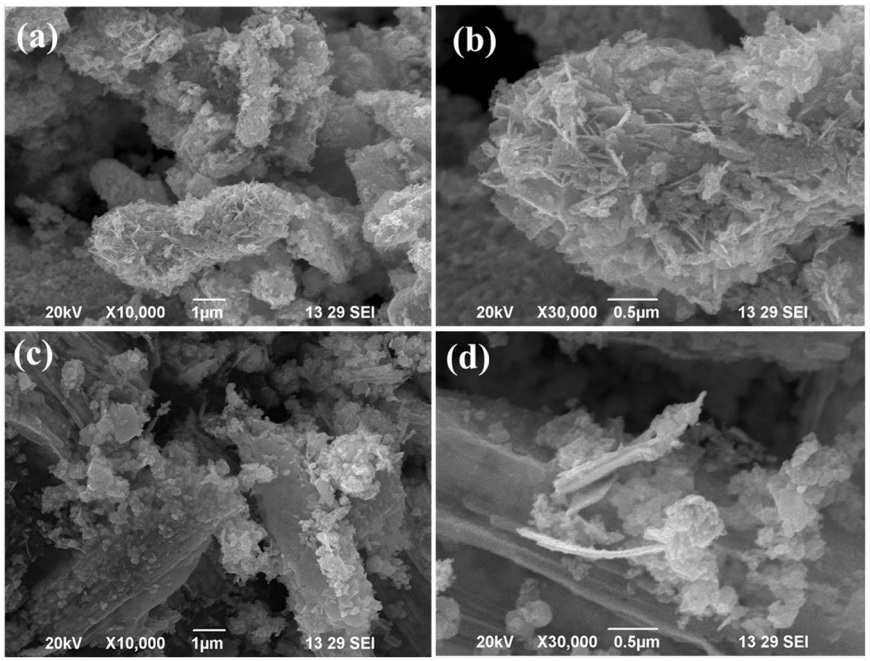

Fig. 3 FE-SEM images of (**a**, **b**) SnO_2, and (**c**, **d**) SnO_2/MWCNT nanocomposites

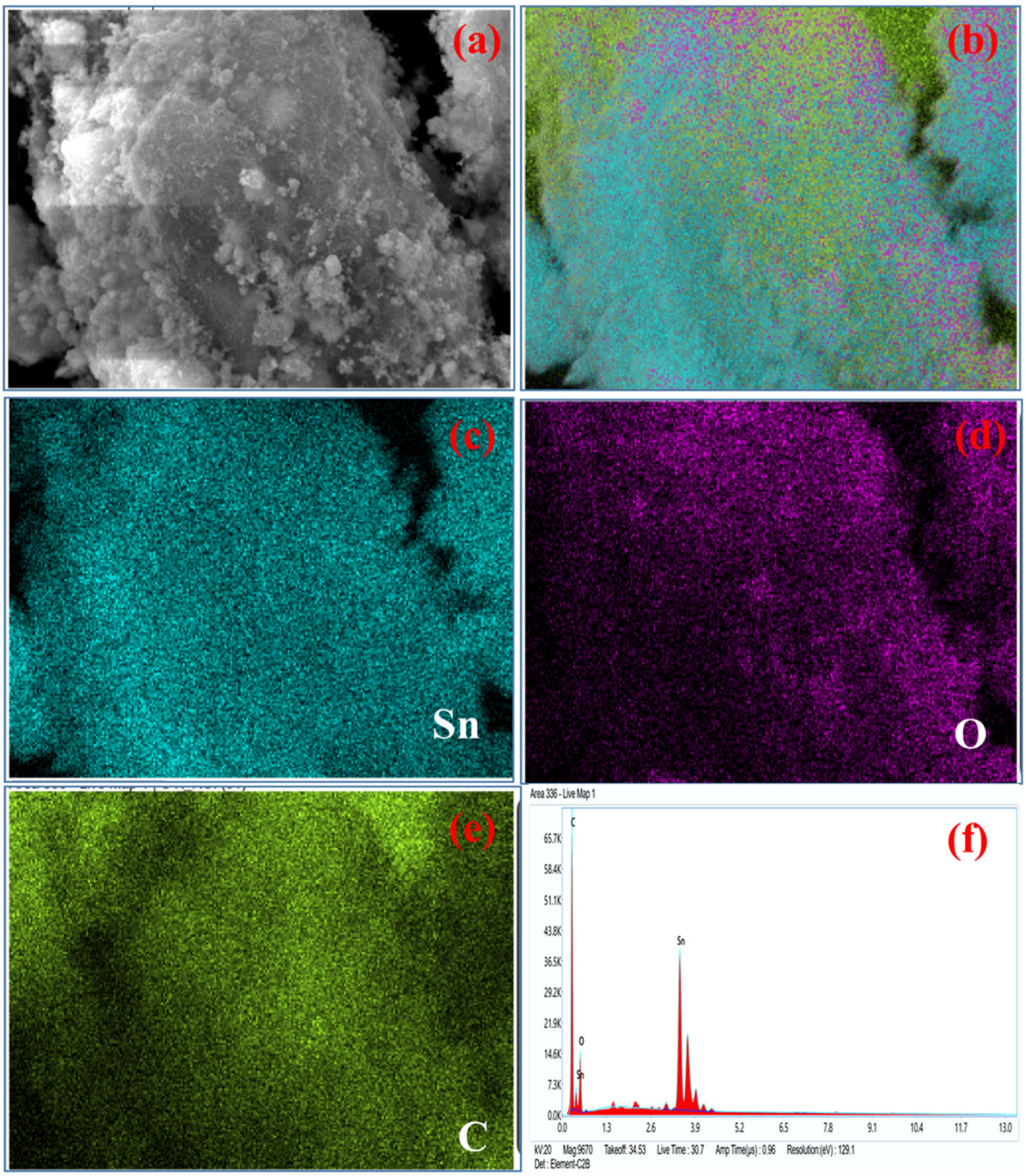

Fig. 4 FE-SEM EDS with mapping images of (**a**–**f**) SnO_2/MWCNTs nanocomposites

potential window, and mass of the active materials (mg) for the three-electrode system.

3 Results and discussion

Figure 1a, shows the XRD patterns of MWCNT were observed at $2\theta = 26.2$ and $2\theta = 44.6$ ° corresponding to (002) and (100) planes of hexagonal structures (JCPDS no. 26–1079). The XRD patterns of SnO_2 and SnO_2/MWCNT nanocomposite were well matched with JCPDS No. 41-1445 in Fig. 1b, c, confirming the presence of the tetrahedral rutile phase. The crystal planes (110), (101), (200), (211), (220), (002), (310), (301), and (110) are represented by the indexed powder XRD patterns with diffraction $2\theta = 26.6°$, 33.9°, 38.1°, 51.7, 55.12°, 58.32°, 62.90° 65.0 and 67.12°, respectively [17]. The diffraction peaks of the SnO_2/MWCNT nanocomposite were similar to the diffraction peaks of SnO_2 with the addition of lower intensity diffraction peaks, confirming the presence of graphitic MWCNT in the SnO_2/MWCNT nanocomposite [18].

The FT-IR spectra of SnO_2 and SnO_2/MWCNT in the 4000–400 cm^{-1} range, as measured at room temperature, are shown in Fig. 2. The main absorption bands at 497 cm

$^{-1}$, and 673 cm^{-1} were assigned to the stretching vibrational modes of the O–Sn–O and Sn–O [19]. In addition, the peaks at 1636 cm^{-1} and 3421 cm^{-1} were related to the bending and stretching vibrations of H-O-H from H_2O molecule absorbed by the SnO_2 surface. Moreover, the absorption peaks of (1640 cm^{-1}), and (1560 cm^{-1}) were as assigned to C = O and C = C in the MWCNT, which confirms the successful formation of the SnO_2/MWCNT nanocomposite [17]. The peaks at 1641 cm^{-1} and 3450 cm^{-1} corresponding to O-H banding and band stretching vibrations of SnO_2/MWCNT nanocomposite.

FE-SEM techniques provided for the visualization of the surface morphologies of SnO_2 and SnO_2/MWCNT nanocomposites. The lower and higher resolution FE-SEM images of SnO_2 showed a dumbbell-like morphology with an average diameter of 2.5 µm, as shown in Fig. 3a, b. The lower and higher magnification FE-SEM images of the SnO_2/MWCNT nanocomposite are also shown in Fig. 3c, d, which also illustrates the irregular rod shape of SnO_2 with MWCNTs having an average diameter of 2 µm. Figure 4a–f shows the FE-SEM with EDS mapping images of SnO_2/MWCNT nanocomposite with the elements Sn, O, and C, and those results indicate the successful formation of SnO2/MWCNT nanocomposite.

Figure 5a, b shows the TEM and HR-TEM images of SnO_2/MWCNTs nanocomposites. The MWCNTs decorated on the SnO_2 nanoparticles (small size of 200 nm), which were attached to the surface of the MWCNT in the SnO_2/MWCNTs composite in Fig. 5a, b. The HR-TEM image revealed two lattice fringes with a spacing of 0.35 nm and 0.36 nm, corresponding to the (110) and (002) plane of SnO_2/MWCNTs nanocomposites.

Figure 6 shows, a three-electrode cell setup using an aqueous electrolyte (1 M KOH) and the characterized the electrochemical energy storage properties of the prepared SnO_2 and SnO_2/MWCNTs electrode materials. These electrochemical techniques included cyclic voltammetry (CV), galvanostatic charge/discharge (GCD), and electrochemical impedance spectroscopy (EIS). The CV curves of prepared SnO_2 and SnO_2/MWCNTs composite electrodes are shown in Fig. 6a, b at different scanning rates of 5, 10, 20, 40, 60, and 80 mV/s in a content potential window of 0–0.5 V. Figure 6c shows the comparative CV curves of the SnO_2 and SnO_2/MWCNT electrodes at a sweep rate of 60 mV/s over the potential range of 0 to 0.5 V. Comparative CV curves for all electrode materials show the different redox couplings that signify the Faradaic redox (battery-type) feature in the alkaline electrolyte [20]. The following

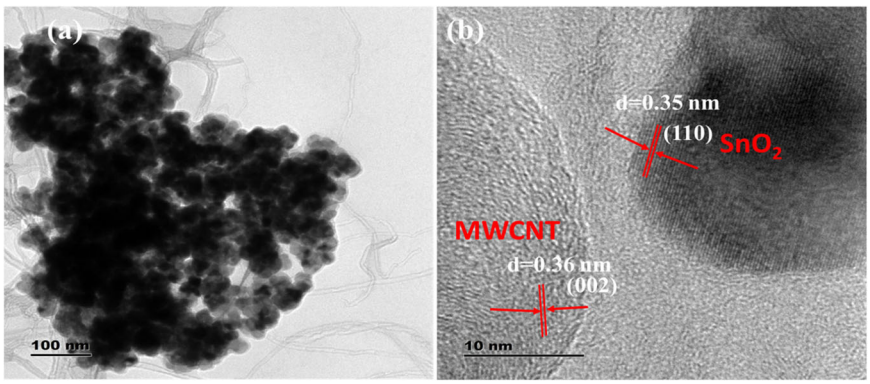

Fig. 5 **a** TEM and (**b**) HR-TEM images of SnO_2/MWCNT nanocomposites

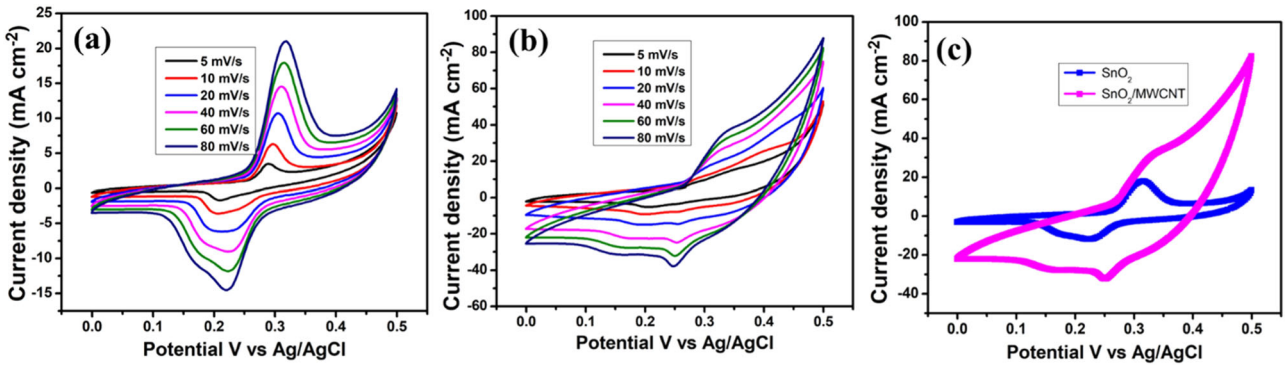

Fig. 6 CV curves of (**a**) SnO_2, (**b**) SnO_2/MWCNTs, and (**c**) comparison CV curves at a constant sweep rate of 60 mV/s

equation possible charge storage mechanism for the electrodes using 1 M KOH as an aqueous electrolyte [21].

$$(SnO_2)\,\text{Surface} + K^+ + e^- \leftrightarrow SnO_2^- - K^+ \quad (2)$$

In addition, the GCD curve of SnO_2, and SnO_2/MWCNTs electrodes with various current densities from 2 to 12 A/g are shown in Fig. 7a, b. The GCD curves of all the prepared electrodes operate in a potential window from 0 to 0.40 V in the three-electrode cell setup (Fig. 7c). Furthermore, the prepared electrodes' nonlinear charge/discharge curves show they all behaved like battery electrodes (faradic battery-type redox) [22].

The calculated specific capacitance of prepared SnO_2 and SnO_2/MWCNTs composite electrodes with various current densities is shown in Fig. 8a. The SnO_2/MWCNT electrodes delivered a maximum specific capacitance of 255 F/g when compared to the SnO_2 electrode at 127 F/g at a current density of 2 A/g. The specific capacitance of the SnO_2/MWCNT composite electrode was compared to that of other electrode materials (Table 1). The SnO_2/MWCNT electrode's improved energy storage ability is attributable to its increased surface area, increased electrochemical active sites, improved electrical conductivity, and synergistic interaction between SnO_2 and MWCNTs in composites.

Figure 8b, c shows the N-q and bode EIS plots of SnO_2 and SnO_2/MWCNT nanocomposite electrodes with equivalent circuits. Table 2 indicates the fitted N-q plot (equivalent circuits) parameters and delivers R_{ct} values of 4.20 Ω and 0.55 Ω corresponding to SnO_2 and SnO_2/MWCNT nanocomposite, respectively. The SnO_2/MWCNT nanocomposite exhibited a lower resistance value compared then pure SnO_2. Moreover, the SnO_2/MWCNT nanocomposite electrode has a cycle life stability of 1,000 GCD cycles at a constant current density of 10 A/g (Fig. 8d). The estimated capacitance retention and coulumbic efficiency of

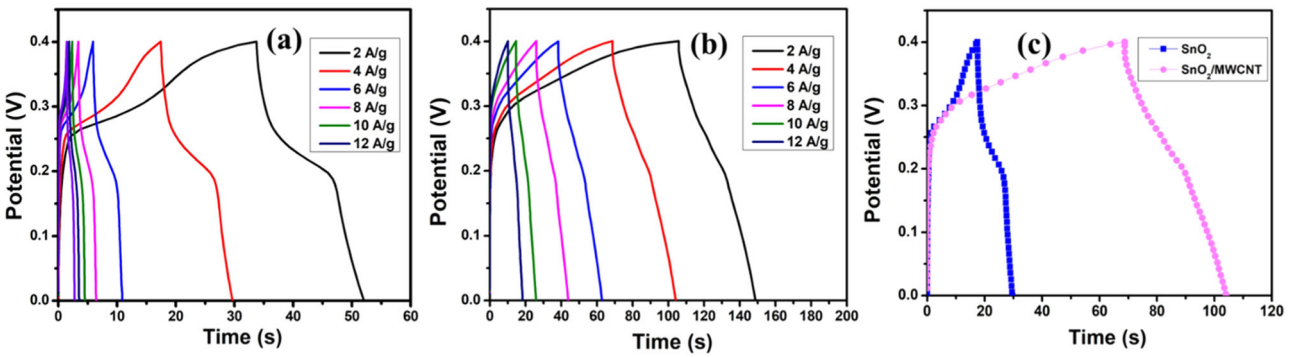

Fig. 7 GCD curves of (**a**) SnO_2, (**b**) SnO_2/MWCNTs nanocomposites, and (**c**) comparison GCD curves of constant current density at 4 A/g

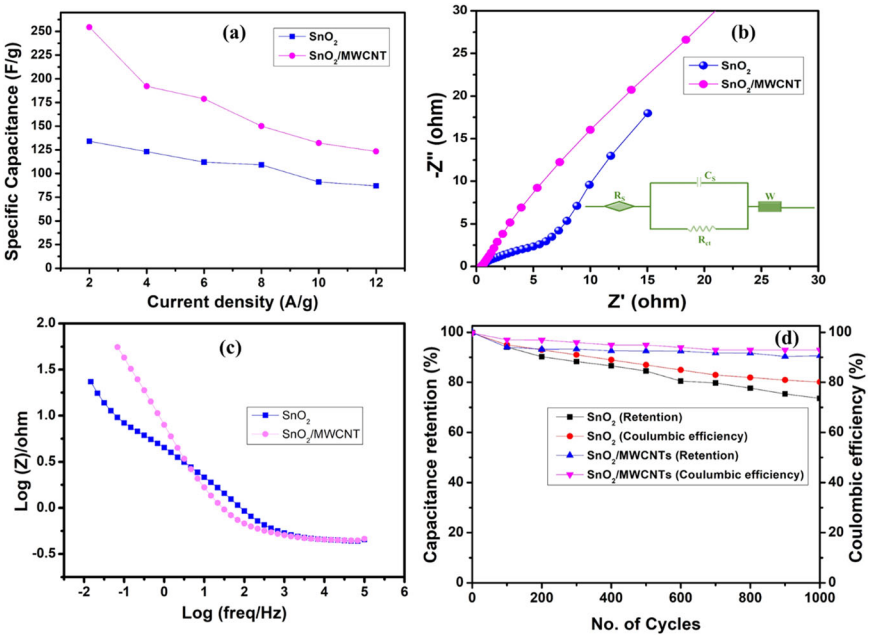

Fig. 8 **a** Specific capacitance with various current densities, (**b**) EIS with equivalent circuit (inserted), (**c**) bode impedance, and (**d**) Cyclic stability, and columbic efficiency of SnO_2 and SnO_2/MWCNTs composite at a constant current density of 10 A/g

Table 1 Comparison of the specific capacitance of the prepared SnO_2/MWCNTs with the previously reported literature

S. No	Electrode Material	Electrolyte	Specific Capacitance	Retention (cycles)	Ref.
1	CuO cauliflowers	1 M Na_2SO_4	179 F/g at 1 A/g	81% (2000)	[24]
2	NiO	1 M KOH	184.6 F/g at 0.5 A/g	93% (1500)	[25]
3	Co_3O_4	1 M Na_2SO_4	182 F/g at 1 A/g	93% (8000)	[26]
4	MXene-MnO_2	1 M Na_2SO_4	104 F/g at 1 A/g	84% (3000)	[27]
5	α-Fe_2O_3/CeO_2 core-shell	2 M Na_2SO_4	158 F/g at 0.5 A/g	87.5% (2000)	[28]
6	FCC@SnO_2	1 M Na_2SO_4	197.7 F/g at 1 A/g	95.5 (5000)	[29]
7	SnO_2/MWCNTs	1 M KOH	255 F/g at 2 A/g	93% (1000)	This work

Table 2 the fitted Nyquist plot (N-q) of SnO_2 and SnO_2/MWCNTs nanocomposites

S. No	Name of the samples	$R_s(\Omega)$	C_s (F. s^{-1})	$R_{ct}(\Omega)$	$W(\Omega\ s^{-1/2})$
1	SnO_2	0.39 Ω	0.34	4.20 Ω	10.11
2	SnO_2/MWCNTs	0.41 Ω	0.79	0.55 Ω	5.23

the SnO_2 and SnO_2/MWCNTs correspond to 76% and 81% and 93%, 95% after 1000 GCD cycles, respectively [23].

4 Conclusion

In summary, a hydrothermal method was used to successfully synthesize SnO_2/MWCNTs nanocomposite, which was used as anode material for a supercapacitor application. The phase purity, crystal structure, functional groups, surface morphology, and internal morphology were studied by XRD, FTIR, FE-SEM, and TEM analyses. The SnO_2/MWCNTs nanocomposite electrode delivered a maximum specific capacitance of 255 F/g at the current density of 2 A/g with a life cycle performance of 93% after 1000 GCD cycles.

Author contributions PJ: methodology, writing - original draft, data curation, visualization. GS: data curation, investigation, software, validation. JD and PS, validation. NB, SR and RU: conceptualization, writing - review & editing.

Compliance with ethical standards

Conflict of interest The authors declare no competing interests.

References

1. Çelik D, Meral ME, Waseem M (2022) Investigation and analysis of effective approaches, opportunities, bottlenecks and future potential capabilities for digitalization of energy systems and sustainable development goals. Electr Power Syst Res 211:108251
2. Sayed K, Abdel-Khalek S, Zakaly HM, Aref M (2022) Energy management and control in multiple storage energy units (battery–supercapacitor) of fuel cell electric vehicles. Materials 15(24):8932
3. Krishan O, Suhag S (2020) Grid-independent PV system hybridization with fuel cell-battery/supercapacitor: optimum sizing and comparative techno-economic analysis. Sustain Energy Technol Assess 37:100625
4. Atchudan R, Pandurangan A, Joo J (2015) Effects of nanofillers on the thermo-mechanical properties and chemical resistivity of epoxy nanocomposites. J Nanosci Nanotechnol 15.6:4255–4267
5. Shaker M, Riahifar R, Li Y (2020) A review on the superb contribution of carbon and graphene quantum dots to electrochemical capacitors' performance: synthesis and application. FlatChem 22:100171
6. Olabi AG, Abbas Q, Al Makky A, Abdelkareem MA (2022) Supercapacitors as next generation energy storage devices: properties and applications. Energy 248:123617
7. Bhojane P (2022) Recent advances and fundamentals of pseudocapacitors: materials, mechanism, and its understanding. J Energy Storage 45:103654
8. Zhang Q, Zhang W-B, Hei P, Hou Z, Yang T, Long J (2020) CoP nanoprism arrays: pseudocapacitive behavior on the electrode-electrolyte interface and electrochemical application as an anode material for supercapacitors. Appl Surf Sci 527:146682
9. Iqbal MF, Ashiq MN, Zhang M (2021) Design of metals sulfides with carbon materials for supercapacitor applications: a review. Energy Technol 9(no. 4):2000987
10. Yin B-S, Zhang S-W, Ke K, Wang Z-B (2019) Advanced deformable all-in-one hydrogel supercapacitor based on conducting polymer: toward integrated mechanical and capacitive performance. J Alloy Compd 805:1044–1051
11. Yang Z, Tian J, Yin Z, Cui C, Qian W, Wei F (2019) Carbon nanotube-and graphene-based nanomaterials and applications in high-voltage supercapacitor: a review. Carbon 141:467–480
12. Cheng F, Yang X, Zhang S, Lu W (2020) Boosting the supercapacitor performances of activated carbon with carbon nanomaterials. J Power Sources 450:227678
13. Veerakumar P, Sangili A, Manavalan S, Thanasekaran P, Lin K-C (2020) Research progress on porous carbon supported metal/metal oxide nanomaterials for supercapacitor electrode applications. Ind Eng Chem Res 59(no. 14):6347–6374
14. Wang Y-X, Lim Y-G, Park M-S, Chou S-L, Kim JH, Liu H-K, Dou S-X, Kim Y-J (2014) Ultrafine SnO 2 nanoparticle loading onto reduced graphene oxide as anodes for sodium-ion batteries with superior rate and cycling performances. J Mater Chem A 2(no. 2):529–534
15. Abou-Elyazed AS, Hassan S, Ashry AG, Hegazy M (2022) Facile, efficient, and cheap electrode based on SnO_2/activated carbon waste for supercapacitor and capacitive deionization applications. ACS omega 7(no. 23):19714–19720
16. Asaithambi S, Sakthivel P, Karuppaiah M, Balamurugan K, Yuvakkumar R, Thambidurai M, Ravi G (2021) Synthesis and characterization of various transition metals doped SnO2@ MoS2 composites for supercapacitor and photocatalytic applications. J Alloy Compd 853:157060

17. Aydın C (2019) Synthesis of SnO_2: rGO nanocomposites by the microwave-assisted hydrothermal method and change of the morphology, structural, optical and electrical properties. J Alloy Compd 771:964–972
18. Zhang Y, Liu M, Sun S, Yang L (2020) The preparation and characterization of SnO_2/rGO nanocomposites electrode materials for supercapacitor. Adv Compos Lett 29:2633366–20909839
19. Ragupathi H, Jarvin M, Nayak AK, Choe Y (2023) Hydrothermal synthesis of SnO_2-rGO nanocomposite from a tea extract for day light driven photocatalyst and supercapacitors N J Chem 4644–4655
20. Geerthana M, Prabhu S, Harish S, Navaneethan M, Ramesh R, Selvaraj M (2022) Design and preparation of ternary α-Fe_2O_3/SnO_2/rGO nanocomposite as an electrode material for supercapacitor. J Mater Sci: Mater Electron 33(no. 11):8327–8343
21. Rani MU, Naresh V, Damodar D, Muduli S, Martha SK, Deshpande AS (2021) In-situ formation of mesoporous SnO_2@C nanocomposite electrode for supercapacitors. Electrochim Acta 365:137284
22. Prabhu S, Sohila S, Navaneethan D, Harish S, Navaneethan M, Ramesh R (2020) Three dimensional flower-like CuO/Co_3O_4/r-GO heterostructure for high-performance asymmetric supercapacitors. J Alloy Compd 846:156439
23. Kumar GS, Reddy SA, Maseed H, Reddy NR (2020) Facile hydrothermal synthesis of ternary CeO2–SnO_2/rGO nanocomposite for supercapacitor application. Funct Mater Lett 13(no. 02):2051005
24. Dubal DP, Gund GS, Lokhande CD, Holze R (2013) CuO cauliflowers for supercapacitor application: novel potentiodynamic deposition. Mater Res Bull 48(no. 2):923–928
25. Duraisamy N, Kandiah K, Rajendran R, Dhanaraj G (2018) Electrochemical and photocatalytic investigation of nickel oxide for energy storage and wastewater treatment. Res Chem Intermed 44:5653–5667
26. Al Jahdaly BA, Abu-Rayyan A, Taher MM, Shoueir K (2022) Phytosynthesis of Co_3O_4 nanoparticles as the high energy storage material of an activated carbon/Co_3O_4 symmetric supercapacitor device with excellent cyclic stability based on a Na_2SO_4 aqueous electrolyte. ACS omega 7(no. 27):23673–23684
27. Wei Y, Zheng M, Luo W, Dai B, Ren J, Ma M, Li T, Ma Y (2022) All pseudocapacitive MXene-MnO_2 flexible asymmetric supercapacitor. J Energy Storage 45:103715
28. Mazloum-Ardakani M, Sabaghian F, Yavari M, Ebady A, Sahraie N (2020) Enhance the performance of iron oxide nanoparticles in supercapacitor applications through internal contact of α-Fe_2O_3@CeO_2 core-shell. J Alloy Compd 819:152949
29. Hong X, Li S, Wang R, Fu J (2019) Hierarchical SnO_2 nanoclusters wrapped functionalized carbonized cotton cloth for symmetrical supercapacitor. J Alloy Compd 775:15–21